Hai-Tao Fan, Hai Wang* and Xiu-Hua Chen

Optimization of multi-sandwich-panel composite structures for minimum weight with strength and buckling considerations

DOI 10.1515/secm-2015-0171
Received April 16, 2015; accepted June 17, 2016; previously published online September 22, 2016

Abstract: A genetic algorithm-based method is proposed to globally optimize the stacking sequence of multi-sandwich-panel composite structures for minimum weight with strength and buckling considerations. The prerequisites for the continuity between sandwich panels are first studied. To implement the summarized continuity rules in the evolutionary optimization, three newly constructed chromosomes are developed to encode the global stacking sequence with no additional repair. Genetic operators, including specialized mutation, swapping and crossover operators, are also developed to effectively explore the design space and keep the continuity rules followed. The Hashin criterion and maximum stress criterion are used to evaluate the strength of sandwich panels. A typical multi-sandwich-panel composite structure with identical and different core thicknesses is optimized to verify the validity and efficiency of the proposed method. It is found that much lighter solutions are obtained with an acceptable efficiency in all cases. It is also found that the weight of the multi-sandwich-panel composite structures can be further reduced when the core thicknesses are not identical.

Keywords: buckling; composite structure; genetic algorithm; optimization; sandwich panel.

1 Introduction

A composite sandwich panel is formed by two laminated faces and a core, which is usually made of the honeycomb or foam material. As a commonly used structural construction, the composite sandwich panel is seen to have great bending stiffness because of its high-stiffness faces separated by the low-density core.

In engineering practices, the composite sandwich structure is known to have great potential in tailor-made design. The different regions in a multi-region sandwich structure are often subjected to different local loads and design constraints. In this paper, these regions are called sandwich panels. Usually, to get solutions with lower weights and fitter stiffness, these sandwich panels are designed to have different but continuous stacking sequences. The corresponding process is known as the design optimization of multi-sandwich-panel composite structures. The design issue involved is the ply drops between the faces of adjacent sandwich panels. As shown in Figures 1 and 2, the sandwich panel *A* and sandwich panel *B* are connected through common plies in their faces (different colors represent plies of different types) and the homogeneous core. In the transition region from *A* to *B*, most plies in the faces of *A* continue, while some plies are dropped.

Because of the discontinuities resulting from the restrictions to the definition of ply orientations and ply materials, the design optimization of the stacking sequences of a composite sandwich panel is always a process full of discreteness [1–16]. In the design optimization of a multi-sandwich-panel structure, the directionality of fiber reinforced plies further raises the continuity requirement on the fiber placement between adjacent sandwich panels. The discreteness, together with the continuity requirement, has made the global stacking sequence optimization of multi-sandwich-panel structures hard to be performed.

Many methods have been developed to optimize the global stacking sequences of multi-panel composite structures [14, 17–33]. Kristinsdottir et al. [18] introduced the term blending and proposed the greater-than-or-equal-to blending rule, in which plies were dropped from the most critical panel, to get the blended solutions. Liu and Haftka [19] developed measures of continuity for two adjacent laminated panels and further used the inequality constraints to enforce the stacking sequence continuity. Then

***Corresponding author: Hai Wang,** School of Aeronautics and Astronautics, Shanghai Jiao Tong University, 200240 Shanghai, People's Republic of China, e-mail: wanghai601@sjtu.edu.cn
Hai-Tao Fan: School of Aeronautics and Astronautics, Shanghai Jiao Tong University, 200240 Shanghai, People's Republic of China; and China Eastern Airlines Corporation Ltd., 200335 Shanghai, People's Republic of China
Xiu-Hua Chen: School of Aeronautics and Astronautics, Shanghai Jiao Tong University, 200240 Shanghai, People's Republic of China

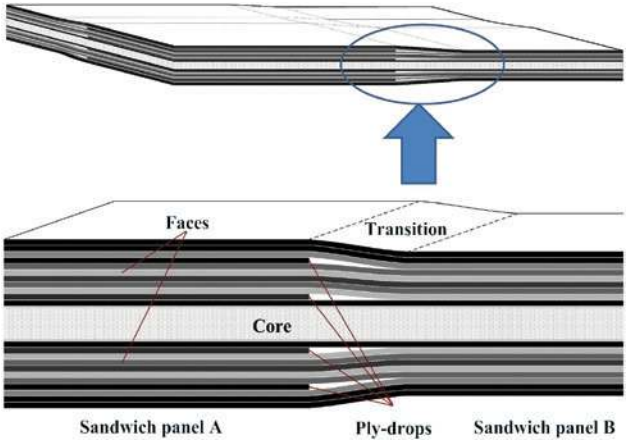

Figure 1: Ply drops between adjacent sandwich panels with identical core thicknesses.

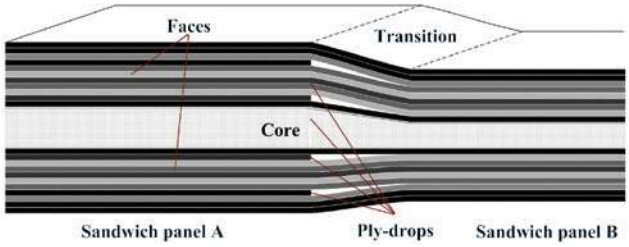

Figure 2: Ply drops between adjacent sandwich panels with different core thicknesses.

their method was demonstrated on a multi-laminated-panel composite wing. Soremekun et al. [20] proposed a sublaminate-based approach for optimizing the multi-panel composite structures with the genetic algorithm (GA). An 18-laminated-panel structure arranged in a horseshoe pattern was optimized and much smaller weight penalties were obtained. Adams et al. [21–23] introduced and implemented the concept of guide-based blending with GA to optimize multi-laminated-panel composite structures. In their method, the stacking sequences of all panels in the whole structure were obtained by deleting contiguous series of plies in a pre-defined guiding stack. By adding one variable per panel of the structure to represent the number of plies dropped from the guide, the continuity requirement was satisfied. Zehnder and Ermanni [24, 25] introduced a patch concept, in which the patch was a layer that covered the arbitrary part of the multi-laminated-panel structure and the stacking sequence of each panel was defined by the order and orientations of the patches. IJsselmuiden et al. [29] presented a multi-step framework for the design of multi-panel composite structures. In their work, the structures were first optimized using panel thicknesses and lamination parameters as continuous design variables. Then the stacking sequence of each panel was obtained using a guide-based GA. Fully blended designs were obtained at a small fraction of the computational cost of traditional blending algorithms. Seresta et al. [30, 31] proposed a multi-chromosomal GA to implement a novel parameterization of the stacking sequence and seamlessly blend stacking sequence across multiple composite panels. Irisarri et al. [32] introduced and implemented the concept of stacking sequence table (SST) with GA for the optimal design of multi-laminated-panel composite structures. The SST was used to describe the sequence of ply drops ensuring the continuity between adjacent panels. Each blended design was represented by an SST and a thickness distribution over the whole structure. Lots of design guidelines which had not been included in previous studies were also considered in their study. Lighter solutions were obtained with the SST method.

Researchers have successfully implemented their methods to optimize the multi-panel composite structures and obtained solutions with great improvements. However, the continuity requirements between laminates are mainly considered in these methods, while the optimizations of multi-sandwich-panel structures are rarely studied. In this paper, the prerequisites for the continuity between two adjacent composite sandwich panels are studied. Then a GA-based method, which follows the continuity rules, is proposed and implemented to globally optimize the stacking sequences of multi-sandwich-panel composite structures.

2 Problem description

In this paper, a ply type is represented by the combination of a ply material and a ply angle. So according to the candidate ply materials and ply angles, the candidate ply types for the optimization can be summarized. For example, the ply type whose material is A and ply angle is θ_1 differs from the ply type whose material is A and ply angle is $\theta_2 (\theta_1 \neq \theta_2)$. The ply type whose material is B and ply angle is θ_1 also differs from the ply type whose material is A and ply angle is θ_1. It is assumed that there are n_{pt} different candidate ply types (PT_1, PT_2, …, $PT_{n_{pt}}$).

In the stacking sequence optimization of a multi-sandwich-panel structure, the first step is to make two sandwich panels continuous to each other. For two composite sandwich panels, their laminated faces should follow some rules to make them continuous. First considering the ply compositions of two adjacent sandwich

panels, the faces of one sandwich panel should not have fewer plies of each type than another sandwich panel. For two adjacent sandwich panels, we can call the sandwich panel with not fewer plies "the parent sandwich panel" and another sandwich panel "the child sandwich panel". For a parent sandwich panel and a child sandwich panel, their common plies in the faces are actually all plies in the faces of the child sandwich panel. Secondly, the common plies of two adjacent sandwich panels should be stacked in the same sequence. This continuity rule is realized by assigning a ranking factor to each ply. The ranking factor of a ply is defined to be a real number whose value determines the position of the ply. For example, there are sandwich panel *A* and sandwich panel *B* in a structure. *A* and *B* have 1 PT_1-type ply (with a ranking factor of 0.2), 1 PT_2-type ply (with a ranking factor of 0.4) and 1 PT_3-type ply (with a ranking factor of 0.6) in common in their faces. In addition, *A* has another PT_1-type ply (with a ranking factor of 0.1) and another PT_2-type ply (with a ranking factor of 0.5). Then after ordering the plies by ranking these factors from small to large, we can get the layups of the face sheets of *A* and *B*. The layup of the face sheet of *A* is $[PT_1/PT_1/PT_2/PT_2/PT_3]$. The layup of the face sheet of *B* is $[PT_1/PT_2/PT_3]$. These ranking factors make the common plies of *A* and *B* stacked in the same sequence.

The two rules are the prerequisites for the continuity between the faces of sandwich panels. The quantities and relative positions of plies with various types should be constrained to follow these rules. Meanwhile the homogeneous core can be seen as a special ply type, which differs from those plies in the laminated faces due to its features as follows.

1. For each sandwich panel, the thickness of the core is variable.
2. The core should be positioned between the two faces of each sandwich panel.
3. For two adjacent sandwich panels, their cores are naturally continuous to each other.

If the core thicknesses in a multi-sandwich-panel structure are identical as shown in Figure 1, the core can be seen as a ply with a variable thickness. If the core thicknesses in a multi-sandwich-panel structure are different as shown in Figure 2, then to realize the global optimization of the core thicknesses, the core can be seen as a group of homogeneous plies with small thicknesses. Here these homogeneous plies are called as core plies. No constraint should be subjected to the quantity and sequence of core plies.

To keep the continuity between adjacent sandwich panels, the continuity rules will be implemented in the GA-based optimization method.

3 Continuity rules-based optimization

3.1 Optimization objectives and constraints

The optimization objective in this paper is to get the lowest weight of a whole multi-sandwich-panel structure, which can be expressed as $\min(\varphi_0)$. However, the discreteness in the optimizations usually leads to the existence of several equally optimal solutions. So on the premise that the lowest weight has been achieved, the largest minimum critical factor (λ_{cr}) across the whole structure is set as the second optimization objective. Here $\lambda_{cr}<1$ represents the failure of the whole structure and larger λ_{cr} represents the safer status. λ_{cr} is determined by the strength failure factor λ_s and the buckling failure factor λ_b. $\lambda_s<1$ represents the strength failure and $\lambda_b<1$ represents the buckling failure. So the critical factor of a sandwich panel can be expressed as

$$\lambda_{cr} = \min(\lambda_s, \lambda_b) \tag{1}$$

For two solutions that have equal weights, the one with the larger λ_{cr} is better.

In the optimization of a multi-sandwich-panel structure, the following constraints are considered.

1. Continuity. The adjacent sandwich panels should be interconnected through the core and continuous plies in the faces. This is the key feature that distinguishes the optimization of a multi- sandwich-panel structure from that of a single sandwich panel.
2. Symmetry. The stacking sequences of the laminated faces should be symmetric about the mid-plane of each panel.
3. Balance. Each sandwich panel should have the same number of θ and $-\theta$ (0 and 90 excluded) plies in its faces.
4. Strength and buckling. The strength and buckling failure should never occur across the whole structure.

The optimization problem of a multi-sandwich-panel structure can be formulated as follows:

$$\text{Minimize } \phi_0 = W \tag{2}$$

Subjected to,

Continuity constraint
Symmetry constraint
Balance constraint
Strength/buckling constraint: $\lambda_{cr}>1$

where *W* represents the total weight of the structure.

To incorporate the buckling and strength constraints, the critical factor λ_{cr} is added into the objective function

through penalty strategies. So the objective function for the optimization of a multi-sandwich-panel structure can be reconstructed as

$$\begin{aligned} &\lambda_{cr} \geq 1, \quad \phi_0 = W + \varepsilon(1-\lambda_{cr}) \\ &\lambda_{cr} < 1, \quad \phi_0 = \frac{W}{\lambda_{cr}^p} \end{aligned} \tag{3}$$

where ε is a small value for rewarding the strength/buckling constraint margin and p is a scaling parameter that controls the searching ability by cutting across the unfeasible design space. Kogiso et al. [4] studied the value of ε and concluded that "too large a value for ε would favor thick designs having a large feasibility margin over the optimum design". It was also concluded that ε should be smaller than $N(c-1)/(c^3-1)$, where $c>1$ and N is the number of plies in a laminate. In this paper, $\varepsilon = 0.089$ and $p = 20$.

3.2 Multi-chromosomal GA

GA has long been used in the optimization of composite structures as an algorithm that can cope well with the discrete optimization problems. However, GA is an algorithm that needs to be designed, which is much more demanding in the optimization of a multi-sandwich-panel structure due to the more difficult handling of constraints. This is reflected in the construction of chromosomes and the design of genetic operators. Among those constraints mentioned above, the handling of the continuity constraint is usually thought to be the most difficult. In this paper, the continuity constraint, together with the symmetry and balance constraints, is incorporated into the chromosome construction.

3.2.1 Chromosomes

Three types of chromosomes, the ply-thickness chromosome, ply-composition chromosome and ply-ranking chromosome, are used to encode the global stacking sequence. The ply-thickness chromosome is constructed to optimize the thickness of thickness-variable plies. The

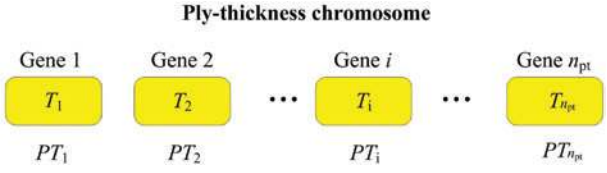

Figure 3: The ply-thickness chromosome.

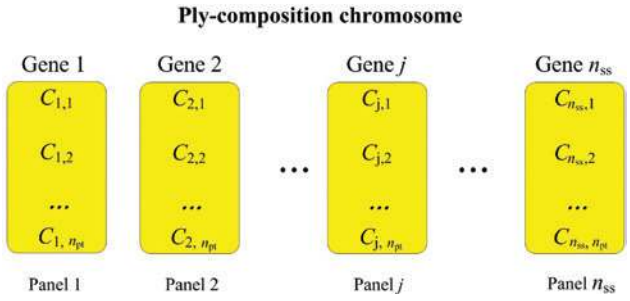

Figure 4: The ply-composition chromosome.

ply-composition chromosome consists of the ply composition information, while the ply-ranking chromosome consists of the ply ranking information.

As shown in Figure 3, the ply-thickness chromosome is defined to be formed by n_{pt} real-coded genes. The ith gene T_i represents the thickness of the ith ply type. For the ply type that has a fixed thickness, the range of the corresponding gene would be restricted to a fixed value.

The ply-composition chromosome helps implement the first continuity rule. As shown in Figure 4, a ply-composition chromosome consists of n_{ss} ply-composition genes. n_{ss} is the number of substructures across the whole structure. Each ply-composition gene, which represents the ply composition of a single sandwich panel, is composed of n_{pt} integer-coded child genes. n_{pt} is the number of ply types. Each integer gene represents the number or half number (for symmetry conditions) of plies of the corresponding type in the corresponding sandwich panel. For example, when subjected to the symmetry constraint, the value of $C_{j,i}$ in Figure 4 represents the half number of plies of the ith type in the jth sandwich panel.

The ply-ranking chromosome implements the second continuity rule. While the ply-composition chromosome determines the ply composition of all sandwich panels, the ply-ranking chromosome could further determine the sequence of these plies to get the full lay-up definition of each sandwich panel. As shown in Figure 5, a ply-ranking chromosome consists of N_{pt} ply-ranking genes.

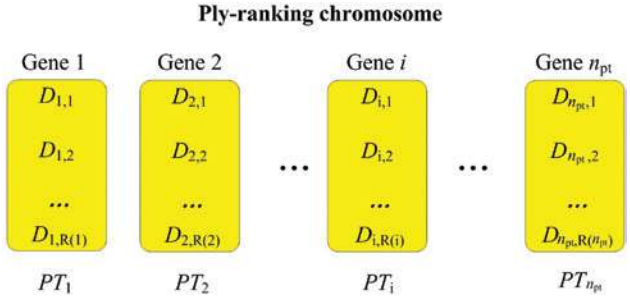

Figure 5: The ply-ranking chromosome.

The *i*th ply-ranking gene represents the ranking factors of PT_i-type plies. Each ply-ranking gene is composed of several real-coded child genes, where the *j*th child gene in the *i*th ply-ranking gene represents the ranking factor of the *j*th PT_i -type ply. The value of these ranking factors is in the range of (0, 1) for ply types that have no special position requirement. For ply types that have special position requirements, the value of the corresponding ranking factor can be set to beyond the range of (0, 1). For example, to keep the core always in the mid-plane of the panels, its corresponding ranking factor can be set as a specified value larger than 1.

It is noted that to incorporate the balance constraint into these chromosomes, two plies with an angle of θ and $-\theta$ ($\theta \neq 0,90$), respectively and the same material can be seen to belong to the same ply type. To incorporate the symmetry constraint, only half of each layup is encoded.

Figure 6 shows how to get the stacking sequence of a multi-sandwich-panel structure by decoding the ply-thickness, ply-composition and ply-ranking chromosomes.

1. We get the value of the *i*th child gene (integer coded) of the *j*th ply-composition gene in the ply-composition chromosome as $c(j,i)$. $c(j,i)$ represents the number of PT_i-type plies in the *j*th sandwich panel.
2. The first $c(j,i)$ ranking factors can be found in the *i*th gene of the ply-ranking chromosome. So we get a group of plies whose ply types and ranking factors are determined. Thirdly, the ranking factors of all plies in the *j*th sandwich panel can be determined.
3. By ordering the plies by these ranking factors, the stacking sequence of the *j*th sandwich panel can be obtained.
4. The thickness of each ply type, which can be found in the ply-thickness chromosome, helps form the full definition of the *j*th sandwich panel.

An example for the decoding of a two-panel sandwich structure can be found in Figure 7. In this example, the ply types in the face sheets are restricted to 0, 45, −45 and 90 plies. The core is discreted to the core plies. The ply-composition chromosome has two genes, which contains

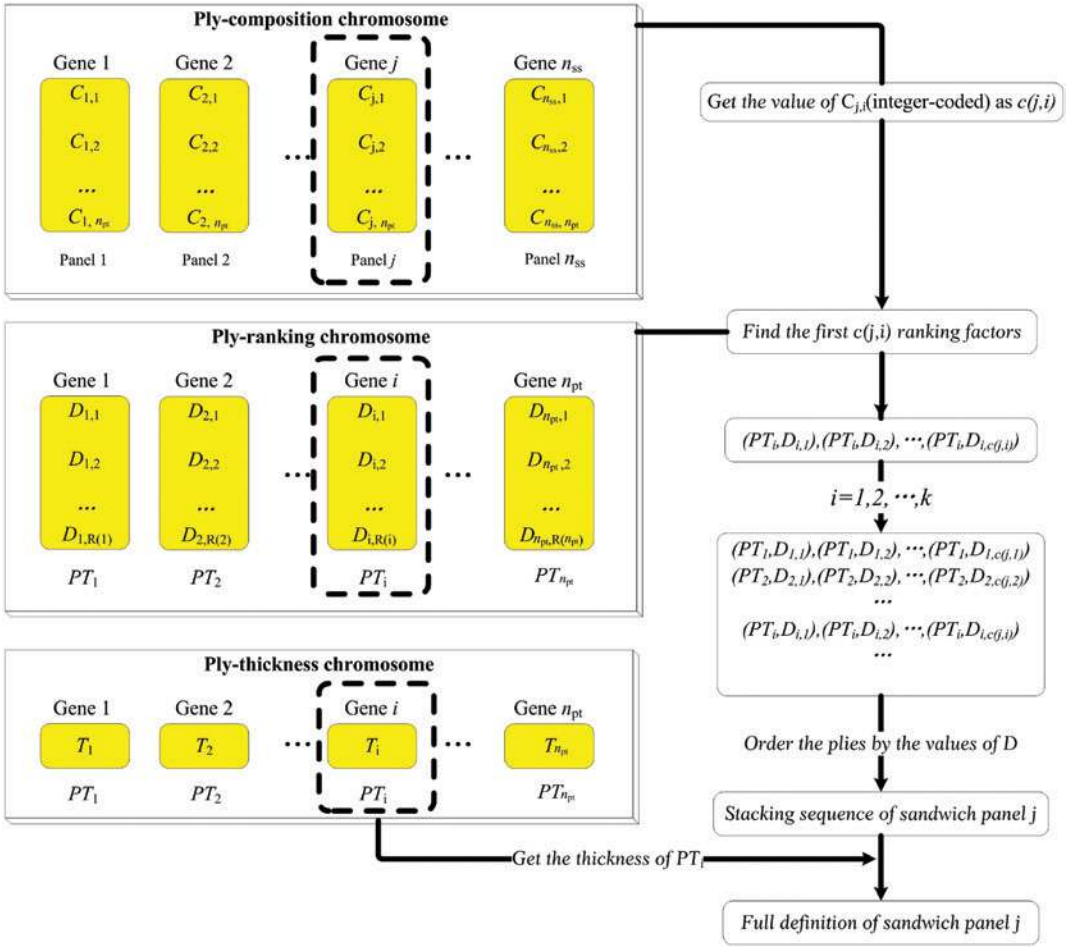

Figure 6: Decoding of chromosomes.

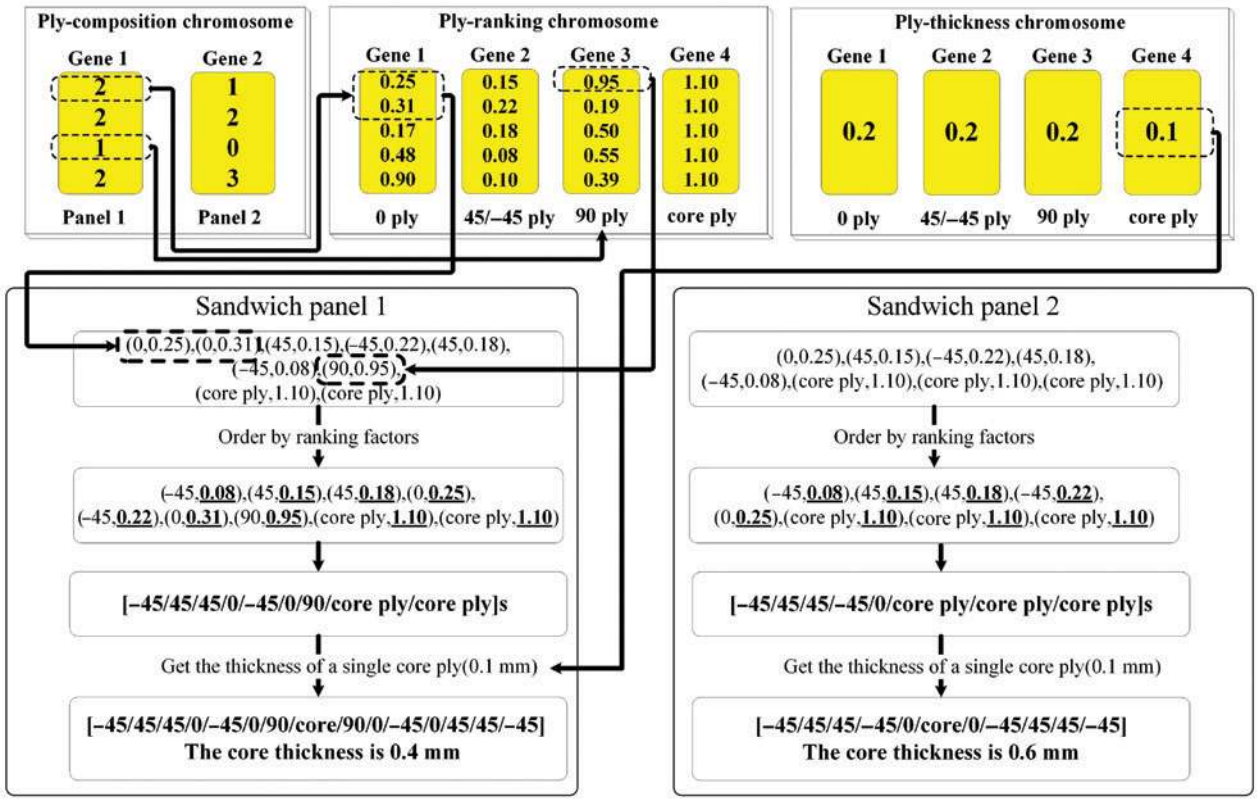

Figure 7: An example for the decoding of chromosomes.

the ply composition information of sandwich panel 1 and sandwich panel 2, respectively. For example, the first integer number in gene 1 is the number of 0° plies in sandwich panel 1, the second integer number in gene 2 is the number of ±45° plies in sandwich panel 2. The ply-ranking chromosome has four genes, which contains the ranking factors of different ply types (0 ply, ±45 ply, 90 ply and the core ply, respectively). The ply-thickness chromosome has four genes, which contains the thicknesses of different ply types (0 ply, ±45 ply, 90 ply and the core ply, respectively). Then we decode the chromosomes as in the figure.

1. From the ply-composition chromosome, we can get the number of 0° plies in sandwich panel 1. The number is 2. Then we get the first and second ranking factors in gene 1 of the ply-ranking chromosome for the first and second 0° plies.
2. Like in step 1, we can get all plies whose ranking factors can be determined.
3. Order these plies by ranking these ranking factors from small to large.
4. Get the layups of sandwich panel 1 and sandwich panel 2.
5. Get the thicknesses of all ply types from the ply-thickness chromosome.
6. Get the core thickness as the sum of the thicknesses of all core plies.
7. Then get the full definitions of all sandwich panels.

The global stacking sequence of the whole structure can be obtained by decoding the chromosomes in this way. The decoded stacking sequences of these sandwich panels are continuous to each other without any additional repair. This means the continuity constraint has been implemented through the constructed chromosomes.

3.2.2 Genetic operators

Three genetic operators, the mutation, swapping and crossover operators, are utilized to match the constructed chromosomes.

The general mutation is implemented on the ply-thickness chromosome and ply-ranking chromosome. This means that in each mutation operation the genes in the ply-thickness and ply-ranking chromosomes are mutated at a specified probability. The new value of each mutated gene is randomly generated in their ranges. In each mutation operation, the ply-composition genes are also mutated at a specified probability. However, due to

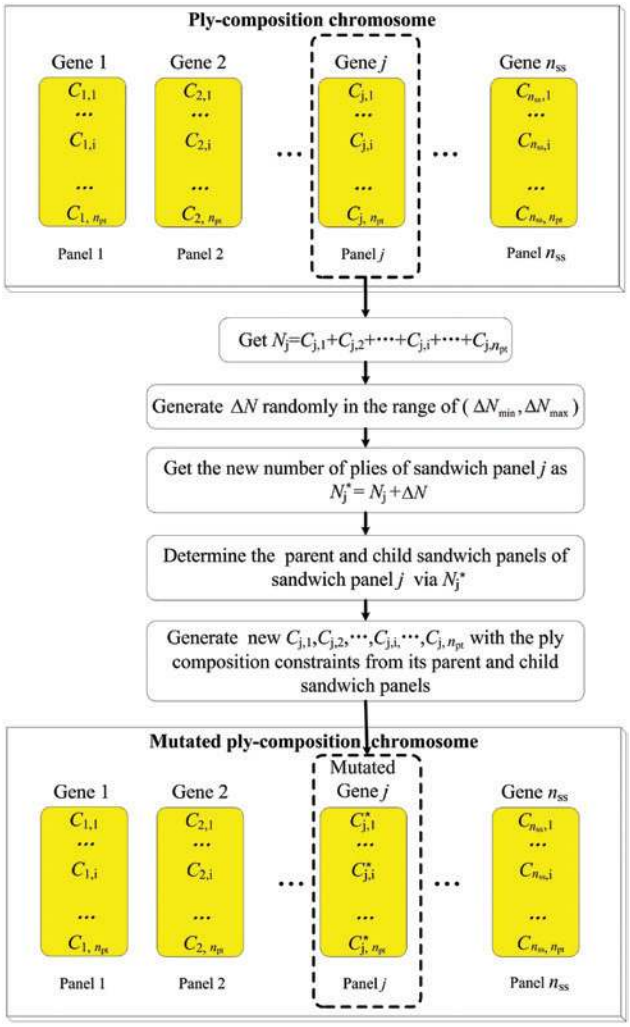

Figure 8: Mutation of a ply-composition chromosome.

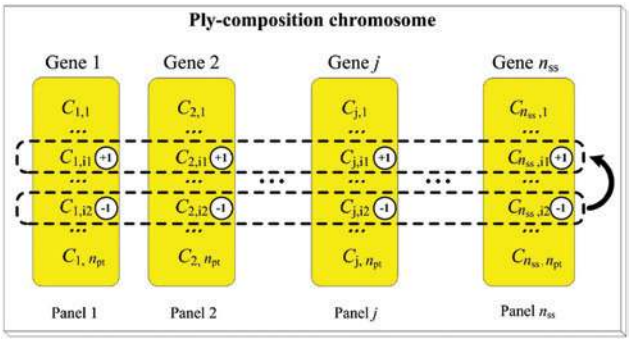

Figure 9: Swapping operations in a ply-composition chromosome.

the continuity constraint, the mutation inside each ply-composition gene differs from that of a ply-thickness gene. As shown in Figure 8, if the jth ply-composition gene is to be mutated, the first step is to mutate the total ply number N_j of the jth sandwich panel. An integer number ΔN is then randomly generated from the range of (ΔN_{min}, ΔN_{max}), where the values of ΔN_{min} and ΔN_{max} are defined to control the mutation range. In the cases of this paper, $\Delta N_{min}=-6$, $\Delta N_{max}=2$. The new total ply number is $N_j+\Delta N$. Once the new total ply number is determined, the parent sandwich panels and child sandwich panels of sandwich panel j can be subsequently determined. According to the ply compositions of parent sandwich panels (or parent ply-composition genes), the upper limit of new $C_{j,i}$ can be determined. Similarly, according to the ply composition of child sandwich panels (or child ply-composition genes), the lower limit of new $C_{j,i}$ can also be determined. On the premise that the new total ply number is located between the lower and upper limits, the new value of $C_{j,i}$ can be randomly determined. In this way, the corresponding sandwich panel of the mutated gene can keep its continuity to the adjacent sandwich panels.

Swapping operations are implemented on both ply-composition and ply-ranking chromosomes. The swapping operation on a ply-composition chromosome is used to swap the ply compositions of the corresponding sandwich panel. The swapping operation is implemented on each ply-composition chromosome at a specified probability. As shown in Figure 9, in each swapping operation, the randomly selected $i1$th child genes of all ply-composition genes swap one or two plies with other randomly selected $i2$th child genes. This means for all sandwich panels some of the PT_{i2}-type plies are changed into PT_{i1}-type plies. Because every time the ply-composition swapping is implemented across the whole structure, the continuities between sandwich panels are preserved. The swapping operation on the ply-ranking chromosome is used to shuffle the location of plies without changing the composition of the sandwich panel. Once the locations of plies change, the flexural properties of the sandwich panels are modified while its in-plane properties are preserved. For each ply-ranking chromosome, the swapping operation is implemented at a specified probability. As shown in Figure 10, in each swapping operation the top k ranking factors of the randomly selected $i1$th ply-ranking

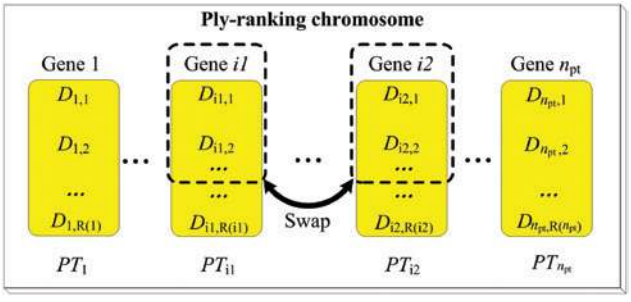

Figure 10: Swapping operations in a ply-ranking chromosome.

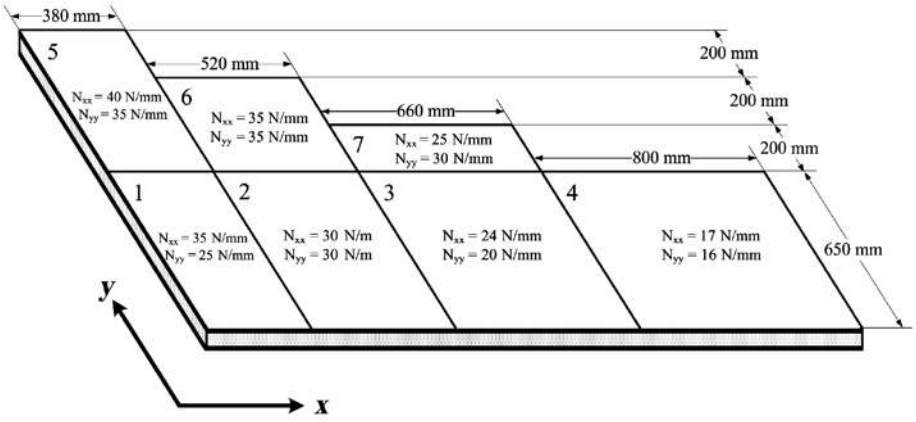

Figure 11: The seven-sandwich-panel structure.

gene swap with the top k ranking factors of the randomly selected $i2$th ply-ranking gene. This means some of PT_{i1}-type plies swap their locations with some of PT_{i2}-type plies in the corresponding sandwich panel.

The crossover operation is implemented on two individuals at a specified probability. Each individual, formed by the ply-thickness, ply-composition and ply-ranking chromosomes, is randomly selected to crossover with another randomly selected individual. In each crossover operation, the chromosomes of individuals are randomly selected to form the new-generation individuals.

The pseudocode for the whole optimization process is as follows:

initialize probabilities for swapping, mutation, crossover genetic operators
generation = 0
initialize Population (generation)
decode and **evaluate** Population (generation)
while termination not detected **do**
apply crossover to Population (generation) giving Children (generation)
apply swapping to Children (generation)
apply mutation to Children (generation)
decode and evaluate Children (generation)
Population (generation + 1) = select from [Population (generation) ∪ Children (generation)]
generation = generation + 1
check for termination
end do

4 Results

Since there is no suitable existing case for the verification of the proposed optimization method, a seven-sandwich-panel configuration is constructed. The dimensions of the panels and the local loadings are shown in Figure 11. The loads are assumed to be fixed. All panels are assumed to be simply supported on their edges. Each panel has two laminated faces and a ROHACELL 51IG foam core. The material of the faces is T300/epoxy, whose properties are listed in Table 1. The properties of ROHACELL 51IG foam are listed in Table 2. The layup of each face is balanced. The layups of the upper face and the lower face are symmetric about the

Table 1: Properties of T300/epoxy material.

Property	
Density, ρ (kg/m^3)	1550
Thickness, t (mm)	0.2
Longitudinal modulus, E_{11} (MPa)	125,000
Transverse modulus, E_{22} (MPa)	8000
Poisson's ratio, μ_{12}	0.3
In-plane shear modulus, G_{12} (MPa)	5000
Longitudinal tensile strength, X_t (MPa)	1600
Longitudinal compressive strength, X_c (MPa)	1000
Transverse tensile strength, Y_t (MPa)	40
Transverse compressive strength, Y_c (MPa)	220
In-plane shear strength, S_{12} (MPa)	80
Through-thickness shear strength, S_{23} (MPa)	60

Table 2: Properties of ROHACELL 51IG foam.

Property	
Density, ρ (kg/m^3)	52
Elastic modulus, E (MPa)	70
Poisson's ratio, μ	0.3
Shear modulus, G (MPa)	19
Tensile strength, X_t (MPa)	1.9
Compressive strength, X_c (MPa)	0.9
Shear strength, S (MPa)	0.8

mid-plane of each panel. For the faces, the minimum number of plies is 14 and the maximum number of plies is 48. The ply orientations in the faces are restricted to 0, ±15, ±30, ±45, ±60, ±75 and 90. The optimization objective is to find a global stacking sequence that minimizes the mass (denoted by M) of the seven-sandwich-panel structure without any failure.

The strength failure of the laminated faces is identified by the Hashin criterion [33, 34], in which the failures of the fibers and matrix are, respectively determined based on their different stress status and failure mechanism. The strength failure factor can be expressed with Hashin's criterion as follows.

1. Fiber mode (λ_s^{fiber} is the strength failure factor of the fibers):
   For tensile conditions ($\sigma_{11} > 0$),

$$\lambda_s^{\text{fiber}} = \frac{1}{\sqrt{\left(\frac{\sigma_{11}}{X_t}\right)^2 + \left(\frac{\tau_{12}}{S_{12}}\right)^2}} \tag{4}$$

   where X_t and S_{12} are the longitudinal tensile strength and the in-plane shear strength, respectively.
   For compressive conditions ($\sigma_{11} < 0$),

$$\lambda_s^{\text{fiber}} = -\frac{X_c}{\sigma_{11}} \tag{5}$$

   where X_c is the longitudinal compressive strength.
2. Matrix mode ($\lambda_s^{\text{matrix}}$ is the strength failure factor of the matrix):
   For tensile conditions ($\sigma_{22} > 0$),

$$\lambda_s^{\text{matrix}} = \frac{1}{\sqrt{\left(\frac{\sigma_{22}}{Y_t}\right)^2 + \left(\frac{\tau_{12}}{S_{12}}\right)^2}} \tag{6}$$

   where Y_t is the transverse tensile strength.
   For compressive conditions ($\sigma_{22} < 0$),

$$\lambda_s^{\text{matrix}} = \frac{1}{\sqrt{\left(\frac{\sigma_{22}}{2S_{23}}\right)^2 + \left[\left(\frac{Y_c}{2S_{23}}\right)^2 - 1\right]\frac{\sigma_{22}}{Y_c} + \left(\frac{\tau_{12}}{S_{12}}\right)^2}} \tag{7}$$

   where Y_c and S_{23} are the transverse compressive strength and the through-thickness shear strength, respectively. The strength failure of the homogeneous core is identified by the maximum stress criterion, with which the strength failure factor of the core can be expressed as

$$\lambda_s^{\text{core}} = \min\left(\left|\frac{X}{\sigma}\right|, \frac{S}{\tau}\right) \tag{8}$$

Table 3: GA parameters.

Population size	100
Probability of mutation of the ply-thickness chromosome	0.14
Probability of mutation of the ply-composition chromosome	0.22
Probability of mutation of the ply-ranking chromosome	0.01 for each gene
Probability of swapping of the ply-composition chromosome	0.20
Probability of swapping of the ply-ranking chromosome	0.20
Probability of crossover	0.05
Termination criterion (generations)	200

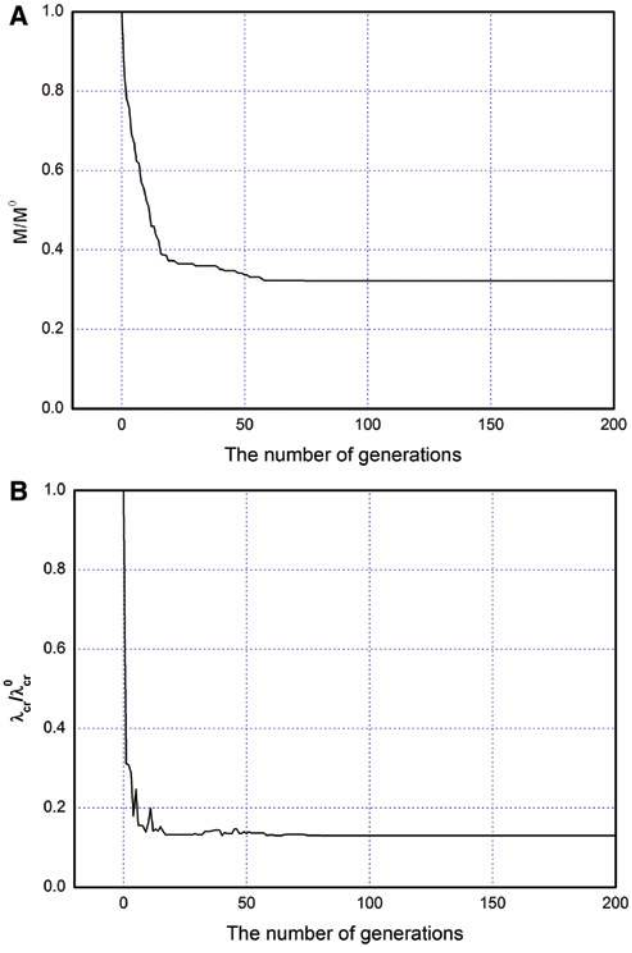

Figure 12: (A) The evolutionary process of the total mass. (B) The evolutionary process of the critical factor. The evolutionary process of design solutions with identical core thicknesses.

where X and S are the tensile/compressive strength and the shear strength, respectively.

Then the strength failure factor of a sandwich panel can be expressed as

$$\lambda_s = \min(\lambda_s^{\text{fiber}}, \lambda_s^{\text{matrix}}, \lambda_s^{\text{core}}) \tag{9}$$

The stress concentration in the transition areas between adjacent sandwich panels is not considered in this paper.

The buckling failure of a sandwich panel, which is subjected to in-plane loads and simply supported on four edges, is identified by the following equation:

$$\lambda_b = \pi^2 \frac{D_{11}(m/a)^4 + 2(D_{12} + 2D_{66})(m/a)^2(n/b)^2 + D_{22}(n/b)^4}{(m/a)^2 N_{xx} + (n/b)^2 N_{yy}} \tag{10}$$

Where λ_b is the buckling factor and $\lambda_b \leq 1$ denotes the occurrence of the buckling failure. a and b are respectively the length and width of the panel. N_{xx} is the force per unit length in the longitudinal (x) direction and N_{yy} is the force per unit length in the transverse (y) direction. m and n are the number of half wavelengths along the x and y directions, respectively. D_{11}, D_{12}, D_{66} and D_{22} are bending stiffness terms of the sandwich panel. The minimum λ_b can be determined by different combinations of m and n. In this study, the minimization over m and n is performed by checking for all values of m between 1 and 10 and all values of n between 1 and 10.

The GA parameters are listed in Table 3. The optimization is implemented by programming in C#. The initial sandwich panels all have 24 ply faces and a 1-mm-thick foam core. The initial stacking sequences are randomly generated. The total mass of the initial seven-sandwich-panel structure is also 31.39 kg. The optimization terminates when the maximum number of generations is achieved.

4.1 Case 1: identical core thicknesses

In this case, the thicknesses of the foam cores in the sandwich panels are identical as shown in Figure 1. The core thickness is restricted to 1–3 mm. The foam core is taken as a foam ply with a variable thickness.

The typical evolutionary process is shown in Figure 12. The total mass and the critical factor of the best design solution reduce rapidly before the 20th generation. Then the total mass reduces slowly between the 20th and 100th generation, while the critical factor fluctuates between 1.000 and 1.128. The lowest total mass is mostly obtained before the 100th generation. The computation time for a run on a PC is about 20 min. So the lowest total mass is mostly obtained on a PC in about 10 min.

Since there are stochastic processes in GA, the convergence speeds in different runs of GA are usually different. So we executed the optimization program for 20 times to observe the convergence process. The lowest total mass obtained in each run is not larger than 10.63 kg. The best result obtained is 10.13 kg, while the corresponding critical factor is 1.000. The detailed optimization results are listed in Table 4. The cross-sections of the optimized solution in the views from the x and y directions, which further demonstrate the continuities in plies of the sandwich panels, can be found in Figure 13. Results show that the sandwich panels obtained in the optimization are continuous to each other. This means the multi-sandwich-panel structures obtained by the proposed optimization method are manufacturable. Meanwhile with identical core thicknesses, the lowest total mass of the seven-sandwich-panel structure obtained in the optimization is 68% lower than the total mass of the initial structure. It is verified that the proposed optimization method can cope well with the optimization of multi-sandwich-panel composite structures with identical core thicknesses.

4.2 Case 2: different core thicknesses

In this case, the thicknesses of the foam core in the sandwich panels are different as shown in Figure 2. The core thickness is restricted to 1–3 mm. The foam core is taken as a group of foam plies with a fixed thickness of 0.1 mm. So the number of foam plies is restricted to 10–30. It is noted that the continuity constraint is not implemented on the foam plies.

The typical evolutionary process is shown in Figure 14. The total mass and the critical factor of the best design solution reduce rapidly before the 20th generation. Then the total mass reduces slowly between the 20th and 30th generation, while the critical factor fluctuates between 1.016 and 1.280. The lowest total mass is mostly obtained before the 50th generation. The computation time for a run on a PC is about 20 min. So the lowest total mass is mostly obtained on a PC in about 5 min.

Similarly, since there are usually differences in the convergences of GA runs, the optimization program was

Table 4: Optimization results for the seven-sandwich-panel structure with identical core thicknesses.

Panel	Stacking sequences (C = core with the thickness of 1.4 mm)																	M (kg)	λ_{cr}
1	[45	−30	30	−30	30	−45		0	C	0		−45	30	−30	30	−30	45]	1.09	1.146
2	[45	−30	30	−30	30	−45	0	0	C	0	0	−45	30	−30	30	−30	45]	1.70	1.025
3	[45	−30	30	−30	30	−45	0	0	C	0	0	−45	30	−30	30	−30	45]	2.16	1.000
4	[45	−30	30	−30	30	−45	0	0	C	0	0	−45	30	−30	30	−30	45]	2.62	1.038
5	[45	−30	30	−30	30	−45		0	C	0		−45	30	−30	30	−30	45]	1.01	1.001
6	[45	−30	30	−30	30	−45	0	0	C	0	0	−45	30	−30	30	−30	45]	1.05	1.197
7	[45		30	−30		−45	0	0	C	0	0	−45		−30	30		45]	0.50	1.318
Total																		10.13	1.000

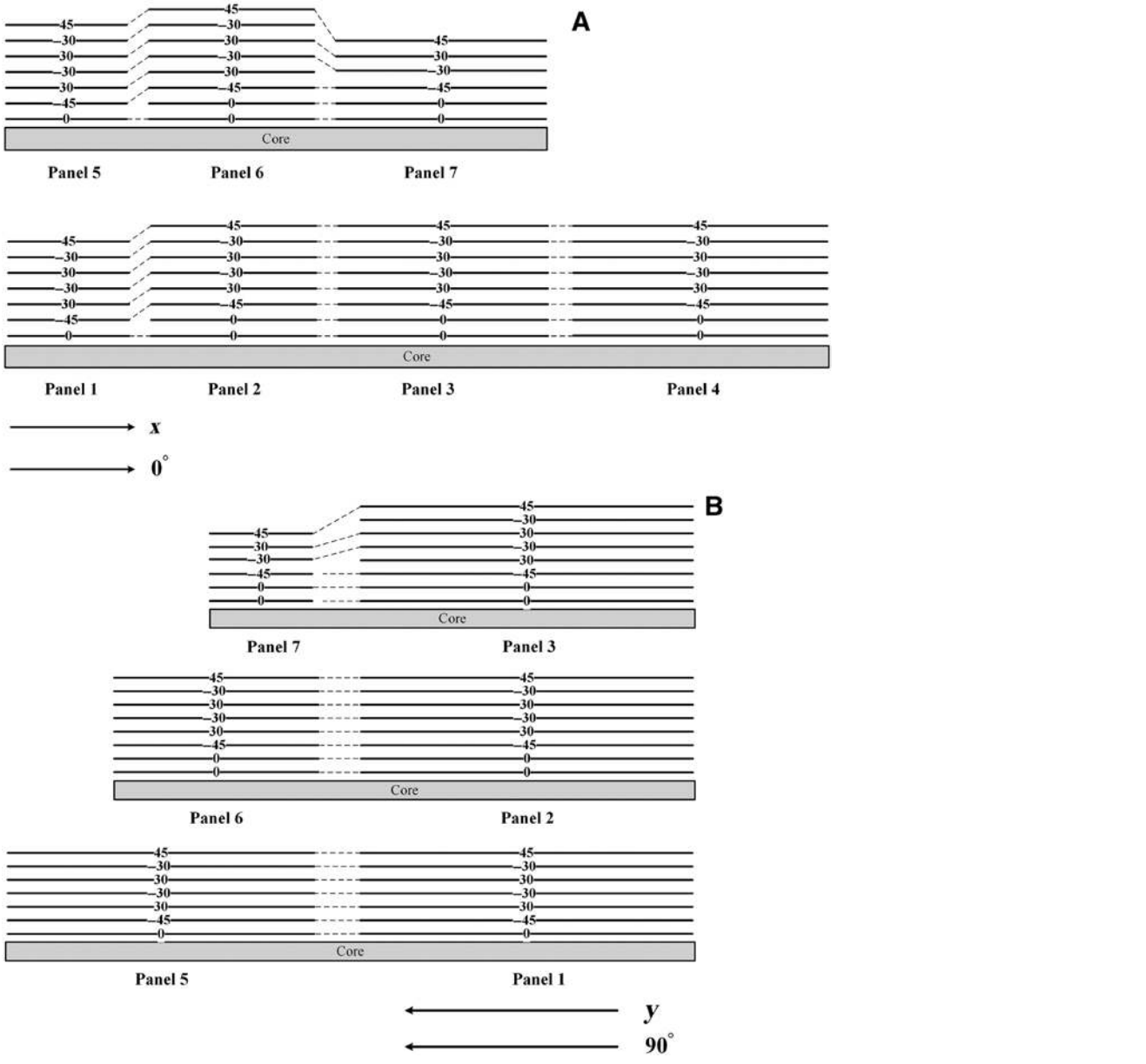

Figure 13: (A) The cross-sections of face sheets in the view from the *x* direction. (B) The cross-sections of face sheets in the view from the *y* direction. The optimization results for the seven-sandwich-panel structure with identical core thicknesses.

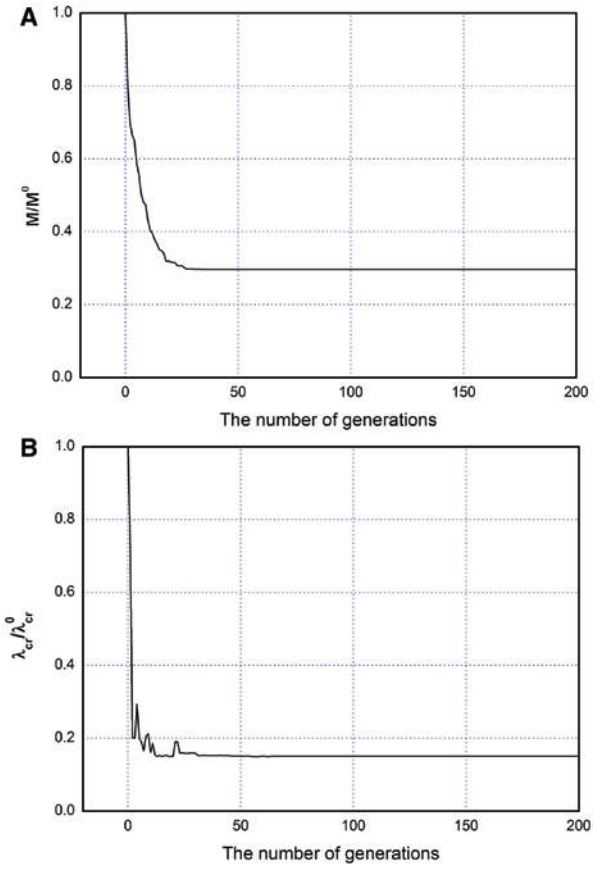

Figure 14: (A) The evolutionary process of the total mass. (B) The evolutionary process of the critical factor. The evolutionary process of design solutions with different core thicknesses.

executed for 20 times. The lowest total mass obtained in each run is not larger than 9.75 kg. The best result obtained is 9.29 kg, while the corresponding critical factor is 1.016. The detailed optimization results are listed in Table 5. Results show that the sandwich panels obtained in the optimization are continuous to each other. This means the obtained multi-sandwich-panel structure with different core thicknesses is manufacturable. Meanwhile the lowest total mass of the seven-sandwich-panel structure obtained in the optimization is 70% lower than the total mass of the initial structure. It is verified that the proposed optimization method can cope well with the optimization of multi-sandwich-panel composite structures with different core thicknesses. The results also show that the lowest total mass of the seven-sandwich-panel structure with different core thicknesses is 8% lower than that of the seven-sandwich-panel structure with identical core thicknesses.

5 Conclusions

In this paper, a GA-based method is proposed and implemented to optimize the global stacking sequence of multi-sandwich-panel composite structures. To explore the design space sufficiently in the optimizations, the prerequisites of the continuity between composite sandwich panels are studied. Then three chromosomes are constructed to include the continuity requirement in the evolutionary optimization of the global stacking sequence. Genetic operators are also designed to keep the diversity and follow the continuity rules. A seven-sandwich-panel composite structure with identical and different core thicknesses is optimized with strength and buckling considerations to verify the efficiency and validity of the proposed optimization method. Results show that the multi-sandwich-panel composite structures with identical and different core thicknesses can be well optimized with an acceptable efficiency. More important, solutions with much lower weights are stably obtained in the verifications. The results also reveal that the total mass of a multi-sandwich-panel composite structure can be further reduced when the core thicknesses are not identical.

Table 5: Optimization results for the seven-sandwich-panel structure with different core thicknesses (T_{core} is the core thickness).

Panel	Stacking sequences(C = core)															T_{core} (mm)	M (kg)	λ_{cr}
1	[−30	45	−45	45	−45	30	0	C	0	30	−45	45	−45	45	−30]	1.3	1.09	1.016
2	[−30	45	−45	45	−45	30	0	C	0	30	−45	45	−45	45	−30]	1.9	1.50	1.049
3	[−30	45	−45	45	−45	30	0	C	0	30	−45	45	−45	45	−30]	1.9	1.90	1.066
4	[−30	45	−45	45	−45	30	0	C	0	30	−45	45	−45	45	−30]	1.7	2.30	1.016
5	[−30	45	−45	45	−45	30	0	C	0	30	−45	45	−45	45	−30]	1.5	1.00	1.025
6	[−30	45	−45	45	−45	30	0	C	0	30	−45	45	−45	45	−30]	1.5	0.92	1.047
7	[−30	45	−45	45	−45	30	0	C	0	30	−45	45	−45	45	−30]	0.9	0.58	1.488
Total																	9.29	1.016

References

[1] Callahan KJ, Weeks GE. *Compos. Part B: Eng*. 1992, 2, 149–160.
[2] Le Riche R, Haftka RT. *AIAA J*. 1993, 31, 951–956.
[3] Kogiso N, Watson LT, Gürdal Z, Haftka RT. *Struct. Optim*. 1994, 7, 207–218.
[4] Kogiso N, Watson LT, Gürdal Z, Haftka, RT, Nagendra S. *Mech. Compos. Mater. Struct*. 1994, 1, 95–117.
[5] Le Riche R, Haftka RT. *Compos. Eng*. 1995, 5, 143–161.
[6] Todoroki A, Haftka RT. *Compos. Part B: Eng*. 1998, 29, 277–285.
[7] Pai N, Kaw A, Weng M. *Compos. Part B: Eng*. 2003, 34, 405–413.
[8] Lopez RH, Luersen MA, Cursi ES. *Compos. Part B: Eng*. 2009, 40, 731–740.
[9] Keller D. *Compos. Struct*. 2010, 92, 2781–2790.
[10] Badalló P, Trias D, Marín L, Mayugo JA. *Compos. Part B: Eng*. 2013, 47, 130–136.
[11] Kim DH, Choi DH, Kim HS. *Compos. Part B: Eng*. 2014, 58, 400–407.
[12] He K, Hoa SV, Ganesan R. *Compos. Sci. Technol*. 2000, 60, 2643–2657.
[13] Mukherjee A, Varughese B. *Compos. Part B: Eng*. 2001, 32, 153–164.
[14] Setoodeh S, Abdalla MM, Gürdal Z. *Compos. Part B: Eng*. 2006, 37, 301–309.
[15] Blom AW, Stickler PB, Gürdal Z. *Compos. Part B: Eng*. 2010, 41, 157–165.
[16] Ghiasi H, Fayazbakhsh K, Pasini D, Lessard L. *Compos. Struct*. 2010, 93, 1–13.
[17] Kim JS, Kim CG, Hong CS. *Compos. Struct*. 1999, 46, 171–187.
[18] Kristinsdottir BP, Zabinsky ZB, Tuttle ME, Neogi S. *Compos. Struct*. 2001, 51, 93–102.
[19] Liu B, Haftka RT. *Proceedings of the 42nd AIAA/ASME/ASCE/AHS/ASC Structures, Structural Dynamics, and Materials Conference*, Seattle, WA, USA, 2001, pp. 16–19.
[20] Soremekun G, Gürdal Z, Kassapoglou C, Toni D. *Compos. Struct*. 2002, 56, 53–62.
[21] Adams DB, Watson LT, Gürdal Z. *Mech. Adv. Mater. Struct*. 2003, 10, 183–203.
[22] Adams DB, Watson LT, Gürdal Z, Anderson-Cook CM. *Adv. Eng. Softw*. 2004, 35, 35–43.
[23] Adams DB, Watson LT, Seresta O, Gürdal Z. *Mech. Adv. Mater. Struct*. 2007, 14, 139–150.
[24] Zehnder N, Ermanni P. *Compos. Struct*. 2006, 72, 311–320.
[25] Zehnder N, Ermanni P. *Compos. Struct*. 2007, 77, 1–9.
[26] Setoodeh S, Abdalla MM, IJsselmuiden ST, Gürdal Z. *Compos. Struct*. 2008, 87, 109–117.
[27] Van Campen JMJF, Seresta O, Abdalla MM, Gürdal Z. *Proceedings of 49th AIAA/ASME/ASCE/AHS/ASC Structures, Structural Dynamics, and Materials Conference*, Schaumburg, IL, USA, 2008, pp. 7–10.
[28] Giger M, Keller D, Ermanni P. *Struct. Multidisc. Optim*. 2008, 36, 289–305.
[29] IJsselmuiden ST, Abdalla MM, Seresta O, Gürdal Z. *Compos. Part B: Eng*. 2009, 40, 329–336.
[30] Seresta O, Gürdal Z, Adams DB, Watson LT. *Compos. Part B: Eng* 2007, 38, 469–480.
[31] Seresta O, Abdalla MM, Gürdal Z. *Proceedings of 50th AIAA/ASME/ASCE/AHS/ASC Structures, Structural Dynamics, and Materials Conference*, Palm Springs, CA, USA, 2009, pp. 4–7.
[32] Irisarri F-X, Lasseigne A, Leroy F-H, Le Riche R. *Compos. Struct*. 2014, 107, 559–569.
[33] Hashin Z. *J. Appl. Mech*. 1980, 47, 329–334.
[34] Echaabi J, Trochu F, Gauvin R. *Polym. Compos*. 1996, 17, 786–798.